BIOCHEMISTRY
including biophysical chemistry & molecular biology

Article

pubs.acs.org/biochemistry

Unprecedented Selectivity and Structural Determinants of a New Class of Protein Kinase CK2 Inhibitors in Clinical Trials for the Treatment of Cancer

Roberto Battistutta,*[,†,‡] Giorgio Cozza,[§] Fabrice Pierre,*[,∥] Elena Papinutto,[†] Graziano Lolli,[†,‡] Stefania Sarno,[§] Sean E. O'Brien,[∥] Adam Siddiqui-Jain,[∥] Mustapha Haddach,[∥] Kenna Anderes,[∥] David M. Ryckman,[∥] Flavio Meggio,[§] and Lorenzo A. Pinna*[,§,†]

[†]Venetian Institute of Molecular Medicine (VIMM), Via G. Orus 2, 35129 Padova, Italy

[‡]Department of Chemical Sciences, University of Padova, Via Marzolo 1, 35131 Padova, Italy

[§]Department of Biological Chemistry, University of Padova, Viale G. Colombo, 35131 Padova, Italy

[∥]Cylene Pharmaceuticals, Inc., 5820 Nancy Ridge Drive, Suite 200, San Diego, California 92121, United States

Supporting Information

ABSTRACT: 5-(3-Chlorophenylamino)benzo[*c*][2,6]naphthyridine-8-carboxylic acid (CX-4945), the first clinical stage inhibitor of protein kinase CK2 for the treatment of cancer, is representative of a new class of CK2 inhibitors with K_i values in the low nanomolar range and unprecedented selectivity versus other kinases. Here we present the crystal structure of the complexes of CX-4945 and two analogues (CX-5011 and CX-5279) with the catalytic subunit of human CK2. Consistent with their ATP-competitive mode of inhibition, all three compounds bind in the active site of CK2 (type I inhibitors). The tricyclic scaffold of the inhibitors superposes on the adenine of ATP, establishing multiple hydrophobic interactions with the binding cavity. The more extended scaffold, as compared to that of ATP, allows the carboxylic function, shared by all three ligands, to penetrate into the deepest part of the active site where it makes interactions with conserved water W1 and Lys-68, thus accounting for the crucial role of this negatively charged group in conferring high potency to this class of inhibitors. The presence of a pyrimidine in CX-5011 and in CX-5279 instead of a pyridine (as in CX-4945) ring is likely to account for the higher specificity of these compounds whose Gini coefficients, calculated by profiling them against panels of 102 and/or 235 kinases, are significantly higher than that of CX-4945 (0.735 and 0.755, respectively, vs 0.615), marking the highest selectivity ever reported for CK2 inhibitors.

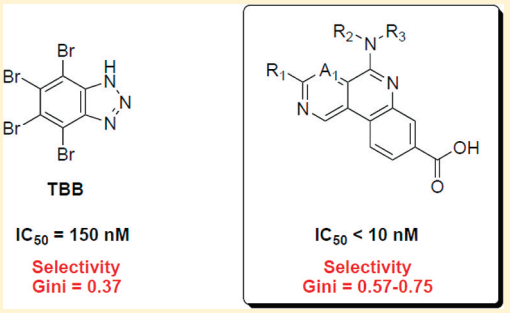

CK2 (an acronym derived from the former misnomer "casein kinase" 2) is a ubiquitous, acidophilic Ser/Thr protein kinase (S/T-x-x-E/D/pS minimum consensus motif) whose most remarkable features are extraordinary pleiotropy[1,2] and "constitutive activity".[3] The latter refers to the fact that the catalytic subunits of CK2 (α and/or α', very similar but encoded by distinct genes) are in an active conformation without the need of any effector or previous phosphorylation, either alone or in combination with the noncatalytic β-subunits to give the heterotetrameric holoenzyme. On the other hand, association with β-subunits may deeply affect the targeting of two subsets of substrates whose phosphorylation is either entirely relying on (class III) or prevented by (class II) the β-subunit.[4] Phosphorylation of class II substrates by the CK2 holoenzyme can be restored by a number of peptidic effectors (including histones and CFTR fragments[5]) through a mechanism whose physiological relevance is still a matter of conjecture.

Although the presence in living cells of catalytic and noncatalytic subunits of CK2 not combined with each other has been repeatedly reported,[6] it is generally held that, unless special circumstances exist, the CK2 activity monitored in biological preparations with the aid of specific peptide substrates[7] is mostly if not entirely due to the holoenzyme. It has been known for a long time that such an activity tends to be particularly high in cancer cells compared to that of their "normal" counterparts, an observation suggesting that, like many other protein kinases, CK2 might be the product of an oncogene. A number of arguments, however, are not consistent with such a view. First, the constitutive activity of CK2 is a property exhibited by this kinase under normal, basal conditions, not the consequence of an oncogenic mutation. Second, no genetic alterations of CK2 are known to cause a gain of function as in the case of typical oncogene-expressed protein kinases. Third, an increase in CK2 activity evokes a

Received: May 31, 2011
Revised: August 25, 2011
Published: August 26, 2011

number of responses, notably resistance to apoptosis,[8] enhancement of the multidrug resistance phenotype,[9] and a strengthened tendency to neovascularization,[10] which altogether "predispose" cells to malignancy. These observations led to the idea that the link between malignancy and an abnormally high level of CK2 found in cancer cells might be explained by the phenomenon of non-oncogene addiction,[11] a term coined to denote overreliance of the tumor phenotype on the overexpression of genes that are not oncogenes in the strict sense of the term.[12]

Consistent with the concept of malignant cells exhibiting non-oncogene addiction to CK2, an ample spectrum of cancer cells derived from tumors of different origin share abnormally high levels of CK2 when compared to those of their normal counterparts;[13] these tumors cells have been shown to undergo apoptosis after treatments, either genetic or pharmacological, that reduce CK2 catalytic activity.[14] Particularly telling in this respect were experiments with cells from multiple myeloma patients whose treatment with CK2 inhibitors induced apoptosis much more effectively than in nonmalignant control cells.[15] Similar observations were also made with cells from T-cell leukemia[16] and acute myeloid leukemia[17] patients. By a complementary approach, CK2 has been shown to afford protection against apoptosis mediated via different pathways (intrinsic and extrinsic).[18]

Consequently, CK2 can be regarded as a prototypical non-oncogene target,[11] and the development of cell permeable selective CK2 inhibitors may not only represent a useful tool for dissecting biological functions mediated by this kinase but also provide a novel therapeutic strategy for counteracting different kinds of malignancies. Many ATP site-directed inhibitors of CK2, with a wide range of potency and selectivity, have already been reported in the literature.[19] More than 20 structures of inhibitors in complex with CK2 have been determined to date, paving the way for the improvement of their potency and selectivity.[20] In particular, it became clear from the first two structures, with emodin and TBB,[21,22] that a unique feature of the CK2 ATP binding site is the small size of a hydrophobic pocket where two bulky residues, V66 and I174, in CK2 replace Ala or other small residues that are found in the majority of protein kinases. More recently, inhibitors targeting structural elements outside of the active site expanded the array of options for modulating the enzyme.[23]

Among ATP-competitive CK2 inhibitors, commercially available polyhalogenated heteroaryl TBB and DMAT have been the most widely used in cell studies. A recent assessment of their inhibitory properties against a relatively large panel of kinases[24] revealed, however, that their selectivity profile was not as great as originally believed. Moreover, an evaluation of these molecules by chemoproteomics[25] suggested that DMAT had off-target effects that could be in part responsible for its ability to induce apoptosis in cancer cells. Taken together, these observations stimulate the search for structurally different inhibitors with higher potency and selectivity.

Recently, the discovery of a novel class of potent tricyclic ATP-competitive CK2 inhibitors allowed the therapeutic targeting of CK2 in humans for the first time. Orally available analogue 5-(3-chlorophenylamino)benzo[*c*][2,6]-naphthyridine-8-carboxylic acid [CX-4945 (Figure 1)] displayed pharmacological properties and an in vivo efficacy suitable for its evaluation in clinical trials for cancer.[26−28] SAR and molecular modeling revealed the structural elements of CX-4945 essential for interacting with the ATP site. This model

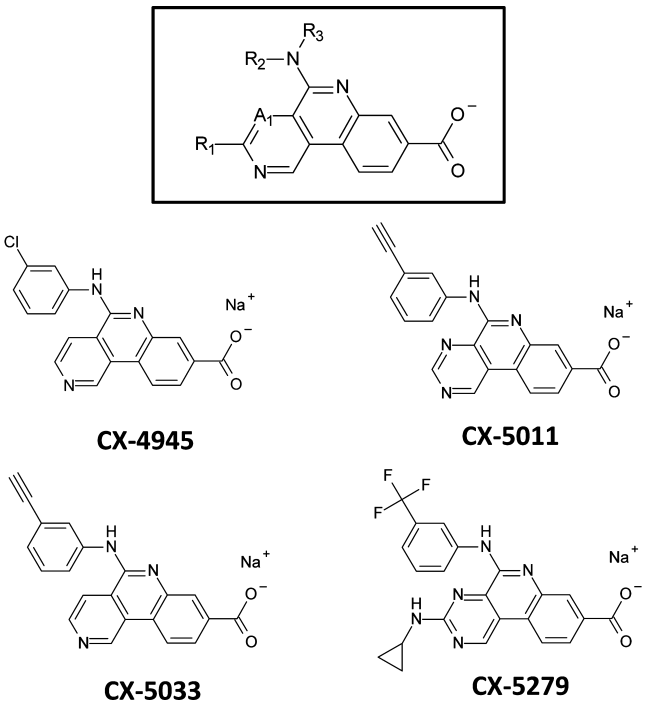

Figure 1. General scaffold (boxed) and structures of the CK2 inhibitors studied here.

encouraged modifications of the pyridine ring of CX-4945 and led to the discovery of various pyrimido[4,5-*c*]quinolones, among which two compounds, 5-(3-ethynylphenylamino)-pyrimido[4,5-*c*]quinoline-8-carboxylic acid [CX-5011 (Figure 1)] and 3-(cyclopropylamino)-5-[3-(trifluoromethyl)-phenylamino]pyrimido[4,5-*c*]quinoline-8-carboxylic acid (CX-5279), were identified as potent CK2 inhibitors.[29]

Herein, we wish to report further characterization of these three potent CK2 inhibitors (CX-4945, CX-5011, and CX-5279), specifically to improve our understanding of their diverging kinase selectivity profiles. These compounds were analyzed for their ability to inhibit native rat CK2 and recombinant human CK2 bearing mutations at V66 and I174. A comprehensive kinase selectivity panel was analyzed, and a comparison with other structurally unrelated CK2 inhibitors was performed. A structure of CX-4945 in complex with CK2 was previously determined by another group at the relatively modest nominal resolution of 2.71 Å [Protein Data Bank (PDB) entry 3NGA[30]]. Herein, we present and discuss a structure of CX-4945, CX-5011, and CX-5279 at a nominal resolution of <2.0 Å that allows a better definition of the interaction with the protein matrix, and in particular the network of crystallographic water that surrounds the inhibitor. We reveal structural components of the molecules that increase their specificity for CK2, providing valuable information that may aid in the design of other classes of CK2 inhibitors and establishing the compounds discussed in this work as the most selective CK2 inhibitors ever reported.

EXPERIMENTAL PROCEDURES

Chemistry. The molecules described here were prepared by Cylene Pharmaceuticals, Inc. Their chemical syntheses were described previously.[26,28]

Kinetic Determination. Human recombinant CK2 ($\alpha\alpha\beta\beta$-holoenzyme) was assayed using a linear enzyme

dx.doi.org/10.1021/bi2008382 | *Biochemistry* 2011, 50, 8478−8488

Table 1. X-ray Diffraction Data Collection and Refinement

	CX-4945	CX-5011	CX-5279
	Data Collection[a]		
X-ray source	XRD1 ELETTRA Synchrotron Light Source, Trieste		
space group	$P2_1$	$P2_1$	$P2_1$
unit cell (Å)	58.5, 46.1, 63.5 (β = 111.6°)	58.5, 46.4, 63.6 (β = 111.7°)	58.4, 46.2, 63.3 (β = 111.5°)
nominal resolution range (Å)	46.1−1.60 (1.69−1.60)	46.4−1.90 (2.00−1.90)	46.2−1.75 (1.84−1.75)
total no. of observations	278706 (39492)	84886 (11363)	80957 (4104)
no. of unique observations	41497 (5905)	24941 (3536)	28551 (2619)
R_{sym}	0.045 (0.466)	0.089 (0.594)	0.083 (0.462)
R_{meas}	0.049 (0.505)	0.106 (0.712)	0.101 (0.620)
R_{pim}	0.019 (0.193)	0.056 (0.387)	0.055 (0.409)
redundancy	6.7 (6.7)	3.4 (3.2)	2.8 (1.6)
mean $I/\sigma I$	24.7 (4.1)	10.9 (2.0)	8.0 (1.6)
completeness (%)	99.2 (97.8)	98.6 (96.5)	89.6 (57.4)
overall B factor from the Wilson plot (Å^2)	19.3	21.9	17.8
	Refinement[a]		
total no. of atoms	3210	3103	3211
no. of waters	392	287	334
resolution range of used data (A)	31.2−1.60 (1.66−1.60)	34.1−1.90 (1.98−1.90)	35.2−1.75 (1.81−1.75)
R_{work} (%)	16.0 (22.2)	17.8 (27.1)	16.0 (23.9)
R_{free}	20.3 (28.0)	22.2 (32.7)	21.1 (30.1)
rmsd for bonds (Å)	0.005	0.007	0.007
rmsd for angles (deg)	0.987	1.057	1.036
average B value (Å^2)			
protein (main chain)	23.4 (20.3)	24.4 (22.8)	22.7 (19.8)
ligand	17.5	17.5	19.7
water molecules	35.4	30.4	32.7
MolProbity validation[37]			
residues in favored regions	97.5%	97.9%	97.2%
residues in allowed regions	100%	100%	100%

[a]Numbers in parentheses refer to data for the highest-resolution shell.

concentration at varying ATP concentrations, ranging from approximately $^1/_{10}$ to 10 times the K_m for ATP for CK2, using Millipore's standard radiometric assay. The following ATP concentrations were used: 1.5, 6, 15, 45, 70, and 155 μM. Two additional ATP concentrations were tested against CX-5011 to aid in K_i estimation (10 and 100 μM). The activity of CK2 was determined at nine concentrations of each compound (CX-4945 and CX-5011) in semilog increments at each ATP concentration. The top inhibitor concentration was 0.1 μM.

CK2 (final concentration of 1.02 nM) was incubated with 20 mM HEPES (pH 7.6), 0.15 M NaCl, 0.1 mM EDTA, 5 mM DTT, 0.1% Triton X-100, 165 μM RRRDDDSDDD, 10 mM magnesium acetate, and [γ-^{33}P]ATP (specific activity of approximately 500 cpm/pmol, concentration as required). The reaction was initiated by the addition of the Mg/ATP mix. After incubation for 40 min at room temperature, the reaction was stopped by the addition of a 3% phosphoric acid solution. Ten microliters of the reaction mixture was then spotted onto a P30 filtermat and washed three times for 5 min in 75 mM phosphoric acid and once in methanol prior to drying and scintillation counting.

All data points were recorded in duplicate, and DMSO controls and acid blanks were included at each ATP concentration. The individual replicates were expressed in terms of the percentage of the DMSO positive control activity. The mean activity (percent control) of each inhibitor concentration was plotted against the inhibitor concentration, and IC_{50} values were determined using GraphPad Prism. The CK2 specific activity measured in the absence of inhibitor (DMSO control) at each ATP concentration was also plotted to indicate the K_m(app) for ATP within the experiment.

Because the extrapolated K_i values using the Cheng−Prusoff equation are similar in magnitude to the concentration of enzyme used in the assay (see ref 27 and Figure S2A of the Supporting Information), both CX-4945 and CX-5011 can be treated as tight binding inhibitors and the Morrison equation for the determination of the K_i values for tight binding inhibitors applied. The concentration of enzyme active sites used in the assays to determine activity in the presence of inhibitor (~1 nM) was significantly less than 200 times the estimated K_i values for CX-4945 and CX-5011 (0.38 and 0.42 nM, respectively), a circumstance that makes graphical determination of the active enzyme concentration inadvisable (see page 314 of ref 31). Therefore, to determine the active enzyme concentration E and the apparent K_i (K_i^{app}) simultaneously at each concentration of substrate (ATP), nonlinear regression analysis of the enzyme activity versus inhibitor concentration was conducted (eq 1), applying the constraint that $E > 0$ (see page 312 of ref 31).

$$Y = V_0\{1 - [(E + X + K_i(1 + [S]/K_m) - \{[E + X + K_i(1 + [S]/K_m)]^2 - 4EX\}^{0.5}) /(2E)]\} \quad (1)$$

where V_0 is the velocity in the absence of inhibitor, E is the active enzyme concentration, [S] is the substrate (ATP) concentration, and K_m = 17.5 μM (K_m for ATP).

dx.doi.org/10.1021/bi2008382|Biochemistry 2011, 50, 8478−8488

Table 2. Kinetic Analysis of Cylene Compounds CX-4945, CX-5011, and CX-5279[a]

compd	name	IC_{50} (nM) nCK2	CK2α	CK2α dm (V66I174AA)	CK2α (V66A)	CK2α (I174A)	PIM1
CX-4945	sodium 5-(3-chloroanilino)pyrido[4,5-*c*]quinoline-8-carboxylic acid	2.50	1.50	15.00	13.5	3.51	216.00
CX-5011	sodium 5-[(3-ethynylphenyl)amino]pyrimido[4,5-*c*]quinoline-8-carboxylate	0.97	2.30	2.07	2.32	2.50	2510.00
CX-5279	sodium 3-(cyclopropyl amino)-5-{[3-(trifluoromethyl)phenyl]amino} pyrimido[4,5-*c*]quinoline-8-carboxylate	2.73	0.91	23.35	13.8	12.5	8520.00

[a]Native CK2 was purified from rat liver.[43] Single and double mutants of the CK2α subunit were generated as reported in refs 39 and 44. CK2 phosphorylation assays were conducted at 37 °C in the presence of increasing amounts of each inhibitor in a final volume of 25 μL containing 50 mM Tris-HCl (pH 7.5), 100 mM NaCl, 12 mM $MgCl_2$, and 0.02 mM [^{33}P]ATP (500−1000 cpm/pmol). The phosphorylatable substrate was the synthetic peptide RRRADDSDDDDD. The reaction was started with the addition of the kinase and was stopped after 10 min by addition of microliters of 0.5 M orthophosphoric acid before aliquots were spotted onto phosphocellulose filters. Filters were washed in 75 mM phosphoric acid (5−10 mL each) four times and then once in methanol and dried before being counted. PIM1 activity was determined by following the same procedure by incubating the kinase in the presence of 50 mM Tris-HCl (pH 7.5), 0.1% (v/v) 2-mercaptoethanol, 0.1 mM EGTA, 30 μM synthetic peptide substrate RKRRQTSMTD, and 100 μM [γ-^{33}P]ATP. Results are means for experiments conducted in triplicate, with the standard error of the mean never exceeding 10%.

The K_i^{app} values thus generated were then plotted versus substrate concentration (ATP) (Figure S2B of the Supporting Information) to determine the K_i values. Using the equation for the determination of K_i values for competitive inhibitors (see page 311 of ref 31), the K_i values were measured as the *Y*-intercept ([ATP] = 0) following linear regression analysis (a single outlier data point for CX-4945 was excluded from the analysis). This gave the following K_i values: 0.223 ± 0.011 nM for CX-4945 and 0.175 ± 0.007 nM for CX-5011.

Kinase Selectivity Panel. The kinase selectivity panels were conducted using the Kinase Profiler service offered by Millipore that utilizes a radiometric filter binding assay. The percent inhibition of each kinase was estimated using 0.5 μM CK2 inhibitor and ATP concentrations equivalent to the K_m value for ATP for each respective human recombinant kinase.

Selectivity Parameters. Lorentzian curves were derived from the selectivity data. Gini coefficients and hit rates were calculated as described in ref 32.

Cell Viability Assay. Various cell lines were seeded at a density of 3000 cells/well 24 h prior to treatment in the appropriate medium and then treated with the indicated concentrations of CK2 inhibitor. Cell suspensions were seeded and treated on the same day. Following incubation for 4 days, 20 μL of Alamar Blue (10% of volume/well) was added, and the cells were further incubated at 37 °C for 4−5 h. Fluorescence with an excitation wavelength of 530−560 nm and an emission wavelength of 590 nm was then measured.

Protein Production, Crystallization, and Structure Determination. After expression in bacterial strain *Escherichia coli* BL21(DE3), recombinant human CK2α^{1-336} was purified by affinity chromatography (HiTrap Heparin HP, GE Healthcare), by anion exchange chromatography (MonoQ, GE Healthcare), and by gel filtration chromatography (Superdex 200 10/300 GL, GE Helthcare). The purified protein in 25 mM Tris, 0.5 M NaCl, and 1 mM DTT (pH 8.5) was concentrated to 9 mg/mL. Inhibitors were preincubated for 5 h before the crystallization drops were set up, mixing 1 μL of 9 mg/mL CK2α^{1-336} with 2 μL of a solution containing a 6-fold molar excess of inhibitors in 2% DMSO. Crystals of the human CK2α^{1-336} complexes were grown by vapor diffusion in 32% (w/v) PEG 4000, 0.2 M Li_2SO_4, 0.1 M Tris, pH 8.5 at 20 °C. Crystals were cryoprotected via addition of 0.5 mL of 30% ethylene glycol to the drop before crystals were frozen. Diffraction data were collected at 100 K on beamline XRD1 of ELETTRA (Trieste, Italy). Data were processed with XDS[33] and scaled with SCALA from the CCP4 suite.[34] Structures were determined with PHASER[35] and refined by alternative rebuilding in COOT[36] and refinement with PHENIX.[37] Data collection and refinement statistics are listed in Table 1. An example of the quality of the final electron density maps for the inhibitors is reported in the Supporting Information (Figure S1).

Molecular Modeling and in Silico Analysis. For the computer-aided molecular docking stages, the crystal structures of the human CK2α catalytic subunit in complexes with CX-4945, CX-5011, and CX-5279 were used. All structures were considered with three water molecules, W1, W2, and W3 (with the exception of the CX-5279 crystal structure, in which W3 is absent), whereas all the other ligands and cofactors were removed. Hydrogen atoms were added to the protein structure using standard geometries with MOE [Molecular Operating Environment (MOE 2010.10), Chemical Computing Group]. To minimize contacts between hydrogens, the structures were subjected to Amber99 force field minimization until the root-mean-square deviation (rmsd) of the conjugate gradient was <0.1 kcal mol^{-1} Å^{-1} (1 kcal = 4.184 kJ; 1 Å = 0.1 nm), keeping the heavy atoms fixed at their crystallographic positions. All the three-dimensional structures of CK2 single and double mutants were treated in the same way shown for the wild type. The in silico mutants were built using MOE Mutate Prompt in combination with a Rotamer explorer Methodology and an Amber99 force field minimization. CX-4945, CX-5011, and CX-5279 were rebuilt using MOE builder and minimized using the PM3 semiempirical quantum mechanics force field implemented in Mopac 7. A set of docking runs were performed both on the CK2αWT three-dimensional structure and on CK2α single and double mutants using Glide. For every docking run, a population of 1000 poses were taken into account; the docking poses very similar to the crystallographic data (rmsd ≥ 1 Å) were defined as "superimposable".

RESULTS AND DISCUSSION

Kinetic Analysis and Selectivity of the New Tricyclic Inhibitors. The structures of the compounds studied here are presented in Figure 1. The benzonaphthyridine compound CX-4945 is the first clinical stage inhibitor of protein kinase CK2 for the treatment of cancer. It is a potent inhibitor of human recombinant CK2 (IC_{50} = 0.001 μM).[26] A number of

dx.doi.org/10.1021/bi2008382|*Biochemistry* 2011, 50, 8478−8488

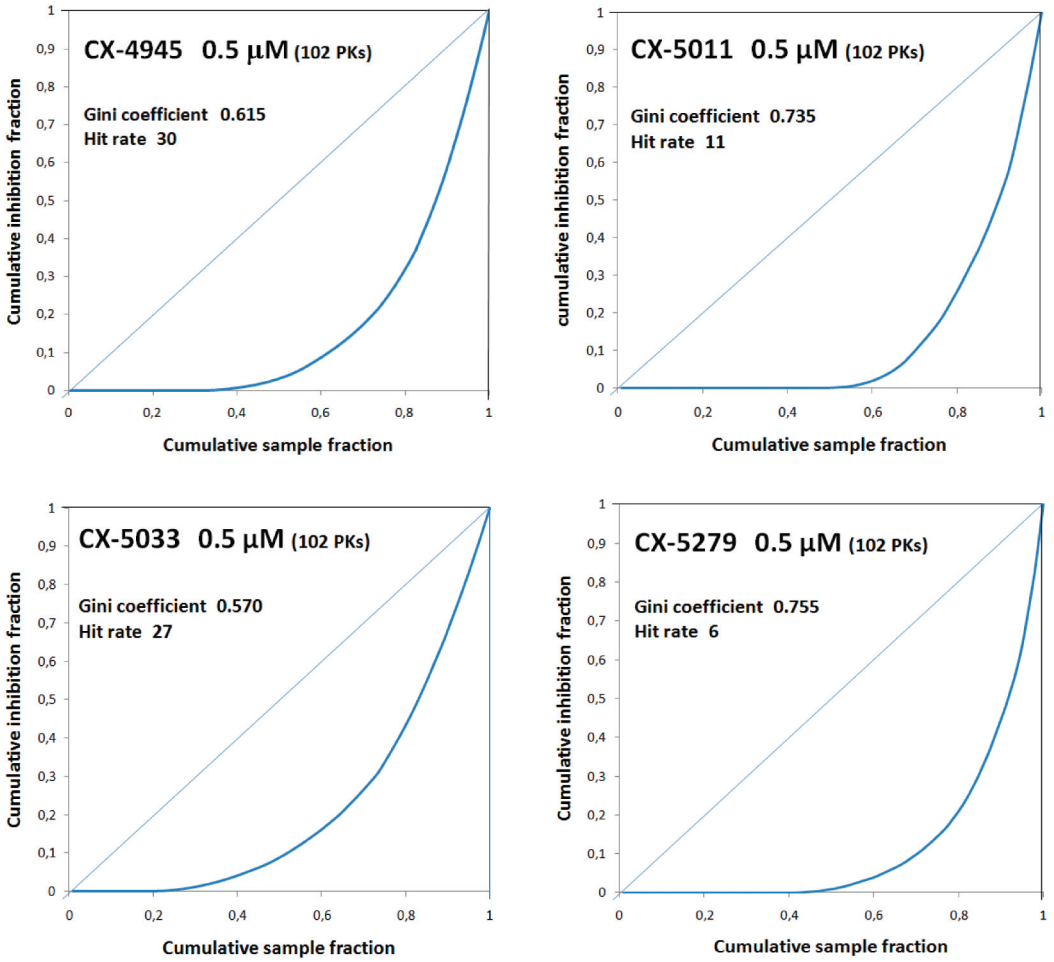

Figure 2. Lorentzian curves, Gini coefficients, and hit rates for compounds CX-4945, CX-5011, CX-5033, and CX-5279. For details, see Experimental Procedures.

substituted congeners were also assayed;[26,29] none of them inhibited CK2 as strongly as CX-4945, which therefore remains the most effective CK2 inhibitor of the series. The replacement of the chlorophenyl group with an acetylenylphenyl group produced a compound (CX-5033) with only a modest reduction in actvity against CK2 (IC_{50} = 0.003 μM).

The effect of replacing the benzonaphthyridine scaffold of CX-4945 with a pyrimidoquinoline, bearing a pyrimidine (two nitrogens) instead of a pyridine (one nitrogen) in the left ring, was also examined by Pierre et al.[26,29] The resulting potent analogue **7e**, here termed CX-5011, and analogue **14k**, here termed CX-5279, displayed activities against CK2 comparable to that of CX-4945, with IC_{50} values of <10 nM.

Compounds CX-4945, CX-5011, and CX-5279 were further analyzed for their ability to inhibit native CK2 (purified from rat liver), the recombinant catalytic α-subunit of human CK2, its double mutant CK2α(V66I174AA), and protein kinase PIM1. The rationale for this analysis stems from previous observations on one hand that Val66 and Ile174 are essential for high-affinity binding of nearly all CK2 inhibitors tested so far and on the other that many CK2 inhibitors tend to inhibit PIM1 as effectively as CK2 itself. As shown in Table 2, IC_{50} values with the native CK2 holoenzyme and with the isolated catalytic subunit are not significantly different either between each other or from those obtained with the recombinant CK2 holoenzyme.[26,29] Interestingly, the V66I174AA double mutation is detrimental to the inhibitory potency of CX-4945 and even more so for CX-5279, while CX-5011 inhibits the double mutant as efficiently as the wild type, a feature never reported before with any specific inhibitor of CK2. Another notable difference among the three inhibitors is elucidated via replacement of CK2 with PIM1 as a target: although none of the new compounds inhibits PIM1 as potently as CK2 (as found instead with many other CK2 inhibitors[24]), PIM1 is sensitive to submicromolar concentrations of CX-4945, but not to CX-5011 (IC_{50} = 2.5 μM) or CX-5279 (IC_{50} = 8.52 μM). Despite their different susceptibilities to the double mutation, both inhibitors CX-4945 and CX-5011 have been shown to be competitive with respect to the phosphodonor substrate ATP, as revealed by plotting their IC_{50} values determined in the presence of various ATP concentrations versus ATP concentration.[26,27] A K_i value of 0.38 ± 0.02 nM was calculated for CX-4945.[27] In the case of CX-5011, the K_i^{app} value was estimated to be 0.42 ± 0.04 nM (Figure S2A of the Supporting Information). Because the values are indicative of a tight binding mode of inhibition, a more precise determination of K_i was performed exploiting the Morrison equation as also illustrated in the Supporting Information (Figure S2B). By this approach, significantly lower K_i values were calculated for both CX-4945 and CX-5011 (0.223 ± 0.011 and 0.175 ± 0.007 nM, respectively).

Although inhibitors CX-4945 and CX-5011 display similar K_i values for CK2 inhibition, the selectivity of the latter is significantly higher, as disclosed by testing the two compounds

dx.doi.org/10.1021/bi2008382 | *Biochemistry* 2011, 50, 8478–8488

against a panel of 102 protein kinases (see Tables S1−S6 of the Supporting Information) and drawing the Lorentzian curves[32] from the resulting selectivity data. These, shown in Figure 2, allow the calculation of a Gini coefficient for CX-4945 (0.615) that is significantly lower than that of CX-5011 (0.735). This analysis was also extended to CX-5033 and CX-5279 (see Figure 2), whose selectivity data are also reported in the Supporting Information. As shown in Figure 2, the latter displays the highest Gini coefficient (0.755) while the former, which shares with CX-4945 the benzonaphthyridine scaffold and with CX-5011 the 3-ethynylaniline group, displays a Gini coefficient (0.570) close to that of CX-4945. This suggests that the higher selectivity of CX-5011 compared to that of CX-4945 results from replacement of the pyridine ring with a pyrimidine ring, and not from the structural changes on the aniline moiety. Such a conclusion is corroborated by calculating the "hit rates", i.e., the number of kinases inhibited by >50% by the four inhibitors using the 102-kinase panel. As also shown in Figure 2, its values are 30 and 27 for CX-4945 and CX- 5033, respectively, while it decreases to 11 and 6 with CX-5011 and CX-5279, respectively, highlighting once more the superior selectivity of the two pyrimidine derivatives.

The precise value of the Gini coefficient, a method for expressing the selectivity of kinase inhibitors against a family of kinases and originally used by economists to measure income inequality, depends on the size and composition of the kinase panel used,[32] ideally becoming an invariant parameter only if it is calculated using the whole kinome (~500 protein kinases). The reliability of the Gini coefficients calculated from a panel of 102 protein kinases can be assessed as the two inhibitors CX-4945 and CX-5011 were further profiled against a larger panel that included 235 protein kinases (almost 50% of the known kinome), and the corresponding Gini coefficients were calculated. As shown in Table 3, these values are very similar to those drawn from selectivity profiles obtained with the panel of 102 protein kinases, thus providing further support for the concept that the Gini coefficient is population-independent for a random selection of kinases. In particular, a panel of ~100 kinases randomly distributed among the kinome appears to be sufficient to provide Gini coefficients for comparative purposes.

Table 3. Gini Coefficients[32] of CK2 Inhibitors Calculated with Various Panels of Protein Kinases

inhibitor	no. of PKs tested	Gini coefficient
CX-4945 (0.5 μM)	102	0.615
CX-4945 (0.5 μM)	235	0.667
CX-5011 (0.5 μM)	102	0.735
CX-5011 (0.5 μM)	235	0.794
CX-5279 (0.5 μM)	102	0.755
CX-5033 (0.5 μM)	103	0.570
quinalizarin (1 μM)[a]	78	0.612
TBB (10 μM)[b]	70	0.375
DMAT (10 μM)[b]	70	0.344
TIBI (10 μM)[b]	70	0.310

[a]From ref 38. [b]From ref 24.

The data presented in Table 3 also highlight the unprecedented selectivity of this new class of CK2 inhibitors whose Gini coefficients are much higher than those of the commonly used commercially available CK2 inhibitors TBB and DMAT, and also significantly higher than that of quinalizarin, recently described as a highly selective inhibitor of CK2.[38] Quinalizarin, however, is much less potent than the new compounds described here with an IC_{50} value of ~50 nM.[38]

From the data in Table 3, we can conclude that (i) all the newly described CK2 inhibitors are more selective than the previously known and commercially available ones and (ii) among the new compounds, CX-5011 and CX-5279 are significantly more selective than CX-4945, although they have similar potency as CK2 inhibitors. This suggests that the change of a pyridine ring (one nitrogen) to a pyrimidine one (two nitrogens) on the left side of the scaffold improves selectivity, probably by weakening interactions with a number of protein kinases other than CK2.

In this respect, it may be worth noting that CX-4945, CX-5011, and CX-5279 display similar efficacy as antiproliferative agents when tested with a variety of cancer cells (Table 4), consistent with the notion that they are cell permeable to a comparable extent. Interestingly, although the EC_{50} values (inhibitor's concentration required to cut cell survival in half) are 3 orders of magnitude higher than the IC_{50} values calculated for CK2 inhibition (Table 2), in the case of CX-5011 and CX-5279 they remain below the in vitro IC_{50} value with PIM1 (also reported in Table 2). These data strongly suggest that the antiproliferative efficacy of these compounds is indeed mediated by CK2. Along with the selectivity data, they highlight the utility of these compounds for the further elucidation of CK2 cellular functions.

Crystal Structures of Human CK2α in Complex with CX-4945, CX-5011, and CX-5279. The starting point for the development of the CX-4945 binding model previously described in ref 26 was the crystal structure of the complex between the maize enzyme and the inhibitor IQA,[39] with which CX-4945 shares some structural analogies. The model was then refined with a SAR analysis of many analogues. The observation that members of this new class of tricyclic CK2 inhibitors not only are extremely potent but also display selectivity that is greater than that of any other CK2 inhibitor described so far prompted us to analyze the structural features underlying their interactions with CK2. We determined the crystal structures of human CK2α in complex with CX-4945, CX-5011, and CX-5279. In the meantime, a structure of the CX-4945 complex has been determined by another group, at the relatively modest nominal resolution of 2.71 Å (PDB entry 3NGA[30]). Here we present and discuss a structure at the much higher nominal resolution of 1.60 Å, with better overall statistics reported in Table 1, i.e., a lower R_{sym} (4.5% vs 7.2%), lower R_{work} and R_{free} values (16.0 and 20.3 vs 18.9 and 21.7, respectively), and a lower average B factor (23.4 Å vs 54.1 Å). The improved structure allows a better definition of the interactions of CX-4945 with the protein matrix and in particular a better characterization of the network of crystallographic water molecules that surrounds the inhibitor, poorly defined in the previous structure. This allows us to improve our understanding of the structural basis of the unpredicted 3-chlorophenyl orientation and the unusual "up" conformation of His160. The reason for these features was not clear on the basis of the previous crystal structure at lower resolution (PDB entry 3NGA), while now they can be nicely explained as discussed below. The structures of the CX-5011 and CX-5279 complexes are also presented, at nominal resolutions of <2.0 Å.

One important structural characteristic of CK2α is the presence of some flexible regions whose functional roles are not

dx.doi.org/10.1021/bi2008382 | Biochemistry 2011, 50, 8478−8488

Table 4. Cell Antiproliferative Activity of CX-4945, CX-5011, and CX-5279

	cell viability IC_{50} (μM)[a]									
compd	HCT-116	MIAPaCa-2	PanC1	BxPC3	PC3	Jurkat	K-562	H1299	MDA-MB-453	MDA-MB-231
CX-4945	2.2	1.1	15.3	4.4	2.1	2.5	5.3	2.4	2.4	6.4
CX-5011	5.6	1.9	9.2	5.9	2.9	2.3	1.6	1.6	3.1	9.8
CX-5279	>10	0.6	2.0	12.0	ND[b]	3.1	0.5	ND[b]	2.2	9.2

[a]Alamar Blue assay; incubation for 4 days with various concentrations of CK2 inhibitors. [b]Not determined.

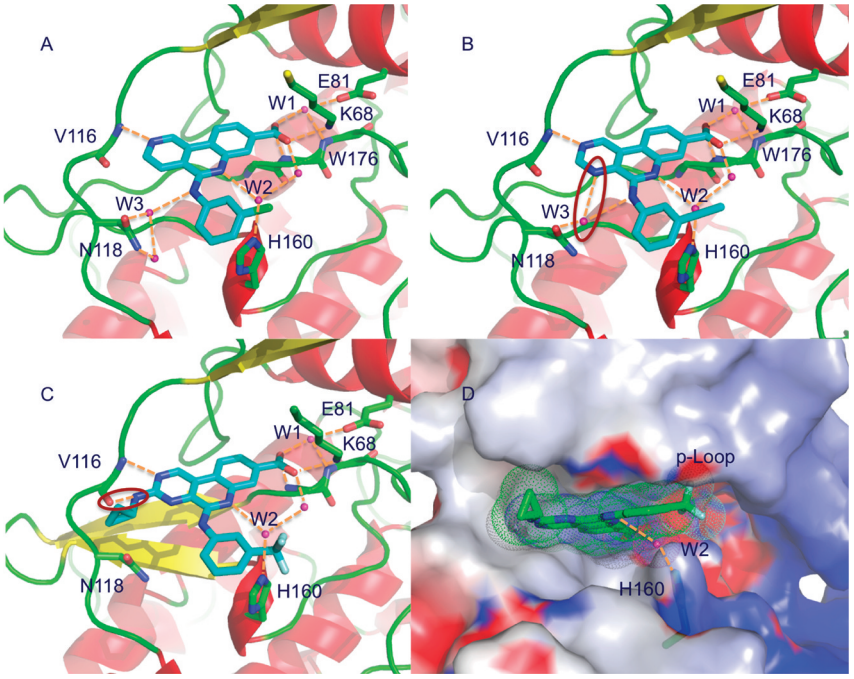

Figure 3. Inhibitors CX-4945 (A), CX-5011 (B), and CX-5279 (C and D) bound to CK2. Hydrogen bonds are represented as dashed orange lines, and water molecules are colored magenta. The three main waters discussed in the text are indicated as W1−W3. In panels B and C, the characteristic H-bonds of CX-5011 and CX-5279, not present in CX-4945, are denoted with a red ellipse. In panel D, the dotted surface of CX-5279 is shown, to highlight the shape complementarity with the CK2 active site. The cyclopropyl is pointing toward the solvent, while the trifluoromethylphenyl is pointing toward the p-loop.

clear yet. These are the region comprising the hinge and the following helix αD (hinge−αD region), the p-loop (or Gly-rich loop), the $\beta4\beta5$ loop, and the side chain of His160 (in the catalytic loop). A striking feature of human CK2α is the flexibility of the hinge−αD region, a unique characteristic among protein kinases.[40] In the isolated α-subunit, this region can be found in an open or closed conformation. In all three complexes presented here, the hinge−αD region is in the open state; as in the case of the complexes with an ATP analogue,[30,40] the p-loop is in the canonical up conformation and the $\beta4\beta5$ loop is bent. The conformation of this loop is different from that in the CX-4945 structure at lower resolution, where it is stretched in a manner similar to that of the tetrameric holoenzyme (note that in ref 30 it is stated that "this region expectedly adopts the closed conformation").

Being ATP-competitive inhibitors, as expected, the three compounds bind in the active site of the enzyme, in a very similar way. It has been predicted that inhibitor CX-5279 could interact slightly differently with the hinge region.[29] As observed in the structures presented here, an almost identical mode of interaction between the three inhbitors and the hinge region of CK2α exists. The binding mode of the three inhibitors is illustrated in Figure 3. All compounds directly interact with the protein matrix by means of a hydrogen acceptor nitrogen (H bound to the amide NH group of Val116 in the hinge region) and of the carboxylic group (bound to both W1 and Lys68, one the five invariant residues in the protein kinase superfamily, which stabilizes the α- and β-phosphates of bound ATP). These general features were previously predicted for CX-4945 by the theoretical model[26] and confirmed by the previous crystal structure (PDB entry 3NGA[30]). The tricyclic scaffold of the inhibitors superposes with the adenine of ATP, establishing extended hydrophobic interactions with the binding cavity. The more extended scaffold allows the carboxylic function to penetrate into the deepest part of the active site, being able to simultaneously interact with the conserved water W1 and Lys68. As highlighted by the SAR data,[26] the negative charge of the carboxylic function plays a fundamental role in the binding. A similar important role is played by the hydrogen acceptor nitrogen bound to the backbone of Val116. Changing the position of this nitrogen has a dramatic effect on the binding constant.[26] The three new structures confirm that the simultaneous presence of the polar interactions established by the properly located nitrogen atom and carboxylic function is essential for guaranteeing the high potency of this class of compounds.

The crystal structures show that one position ortho of the carboxylic function is located very close to Phe113 (the so-

dx.doi.org/10.1021/bi2008382 | Biochemistry 2011, 50, 8478−8488

called "gatekeeper" residue) and Ile95, both in hydrophobic region I (definition according to the pharmacophore model of the ATP-binding site[41]). Accordingly, the insertion of a methyl group at this position is not tolerated, as indicated by the dramatic loss of potency of those analogues.[26] Conversely, the other ortho position has enough space to host a methyl function without compromising the affinity.

In the theoretical model of CX-4945 binding, the 3-chlorophenyl moiety points toward the C-terminal lobe, while in the crystal structures, it is oriented toward Gly46 in the p-loop of the N-terminal lobe (Figure 3A). This is the main difference between the predicted and experimentally determined binding mode. The reason for this 3-chlorophenyl orientation was not completely clear on the basis of the previous crystal structure (PDB entry 3NGA), while it can be nicely explained on the basis of the new one. The nitrogen ortho to the 3-chlorophenylamino substituent forms a hydrogen bond with a water molecule that in turn is bound to the Nε atom of His160, which adopts an unusual up conformation (characterized by a χ_1 torsional angle of approximately 180°). Usually, the His160 side chain is rotated away from the ATP-binding site, in a so-called "down" conformation (χ_1 torsional angle of approximately −80°), as in the structure used for the modeling (PDB entry 1JWH). However, sometimes, specific ligands such as inhibitors quinalizarin and emodin, as well as ATP analogues, can stabilize the up conformation, as in this case. This His160 up orientation hinders the downward rotation of the chlorophenylamino group in position R2 (Figure 3). The similar IC_{50} values of compounds having in position R2 a 3-chlorophenyl or a 3-acetylenylphenyl (CX-5011) or a 3-CF_3-phenyl[25,28] indicate that these substituents of the phenyl ring pointing toward the p-loop have a similar effect on potency. Indeed, the p-loop has an intrinsic flexibility[20] and is able to accommodate the three different substituents equally well (Figure 1). This is not possible in the case of PIM1, where the phenylalanine of the p-loop is pointing toward the active site, in a position that superposes with that occupied by the substituted phenyl of the inhibitors in the CK2 complexes. Most probably, this is the reason for the low potency of these compounds against PIM1, and this is corroborated by the fact that the increase in the phenyl substituent bulkiness corresponds to a decrease in potency. In this particular case, therefore, the selectivity is correlated with this part of the compounds, not to the presence of the pyrimidine (CX-5011 and CX-5279) instead of the pyridine (CX-4945) ring, as suggested above. This is also in agreement with the similar activity against PIM1 of CX-5011 and CX-5033 in the kinase selectivity panel (see the Supporting Information; both diplay ∼70% inhibition at 0.5 μM).

The group in position R1 (Figure 1) is critical for the potency of quinoline inhibitors. The structures of CX-5011 and CX-5279 show that this position is close to the backbone C═O group of Val116, and therefore, only a proper hydrogen bond donor can be accommodated here, such as *c*-PrNH in CX-5279. Conversely, a methyl group, a dimethyl amine, or an ethyl ether (EtO) in position R1 drastically increases the IC_{50}.[26,29] However, this additional direct interaction with the protein matrix seen in CX-5279 is not able to improve the inhibitor potency, as indicated by the similar IC_{50} of CX-5279 and a derivative lacking the *c*-PrNH group in R1.[26,29] The cyclopropyl group is accommodated near His115 toward the bulk of the solvent, without significant steric clashes (Figure 3C,D). The second nitrogen in position A1 of CX-5011 (Figure 1) binds to the side chain of Asn118 from the hinge region via a water molecule that in turn is bound to the phenylamino NH group. However, this interaction does not cause an increase in potency, as indicated by the comparison between the IC_{50} values of CX-5011 and CX-5033, and between those of CX-4945 and a derivative with a nitrogen in position A1.[26,29]

Previously, several low-molecular weight inhibitors were crystallized in complex with CK2.[20] On the basis of these crystal structures, it was recognized that fundamental features of an ATP-competitive CK2 inhibitor are appropriate hydrophobicity, excellent shape complementarity with the unique and small active site, and the ability to establish polar interactions with both the two main anchoring sites, the Val116 backbone at the beginning of the hinge region and the positive electrostatic area near the conserved water W1 and Lys68. The new inhibitors have all these features at their best, and essentially, this is the rationale for their high potency.

The extended network of water molecules surrounding the inhibitors, revealed by these three new structures, can provide important clues for the further development of these compounds.

In drug discovery, thermodynamic binding parameters determined by the isothermal titration calorimetry technique (ITC) can be very informative, particularly when coupled to information about three-dimensional structure.[42] For the inhibitor CX-4945, such thermodynamic data for binding to the human CK2 enzyme are available in the literature,[30] so we can take advantage of our high-resolution crystal structure to interpret them and to derive hints for further development of other CK2 inhibitors. ITC analysis confirms a very strong binding of CX-4945 to the human enzyme, with a K_d of <10 nM.[30] The binding is dominated by a strong enthalpic contribution (ΔH° = −56.8 kJ/mol), with a slightly negative (unfavorable) $T\Delta S^\circ$ term of −9.6 kJ/mol. This implies that the hydrophobic interactions, characterized by a strong favorable entropy, are not the main factor responsible for the binding. Given the extended hydrophobic nature of the inhibitor and of the binding site, the negative $T\Delta S^\circ$ suggests that other unfavorable entropic contributions must be taken into account and that the latter are able to overcome the gain in entropy expected from the hydrophobic contribution. An unfavorable entropic term is commonly due to conformational changes in the ligand and/or in the protein upon binding. In our case, both are possible. In the inhibitor, there are two torsional angles free to rotate around the disubstituted amino function, and as seen above, CK2α shows elements with a relevant conformational plasticity around the binding site. In this case, particularly relevant are the p-loop and His160, whose intrinsic flexibility is strongly reduced upon ligand interaction. The reduction of these degrees of freedom due to inhibitor binding (via a "conformational selection" rather than an "induced fit" mechanism) can, at least partially, counteract the favorable entropy associated with the hydrophobic interactions, with the final result of a slightly unfavorable (negative) $T\Delta S$ term. An unfavorable entropic contribution can also derive from the loss of the degree of freedom for the crystallographic waters surrounding the inhibitor (Figure 3).

The strong enthalpic contribution, essential for CX-4945 binding, is indicative of strong noncovalent interatomic interactions. The crystal structure reveals that there are two major polar interactions, the hydrogen bound to Val116 and the electrostatic interaction with Lys68. The removal of one of these interactions or the other causes a dramatic decrease in the

dx.doi.org/10.1021/bi2008382 | *Biochemistry* 2011, 50, 8478–8488

inhibitor affinity,[26] and therefore, we can conclude that they are principally responsible for the favorable enthalpic term. Because of the good shape complementarity between the inhibitor and the binding site, we can also speculate that the van der Waals interactions make a significant contribution to the enthalpy of binding. The substitution of the carboxylic function of the inhibitor with an amide group, still able to form hydrogen bonds with the protein matrix, increases the IC_{50} from 1 to 417 nM.[26] This indicates that the enthalpic contribution of the carboxylate to the binding is due primarily to the electrostatic nature of the interaction with Lys68, not to its hydrogen bond capability.

We can conclude that the thermodynamics of binding of CX-4945 to CK2 is dominated by an enthalpic term mainly due to the hydrogen bond to Val116 and to the electrostatic interaction with Lys68, while the conformational selection mechanism of binding, at the level of both the inhibitor and the protein active site, plays an unfavorable entropic role. A possible improvement in this class of inhibitors would be the removal of the rotational freedom around the amine function.

An intriguing question arising from the structures of the CX-4945 and CX-5011 complexes in which the two inhibitors are almost perfectly superimposed is why their binding displays different susceptibilities to the replacement of V66 (in the adenine region) and I174 (in the hydrophobic region I) with alanine (see Table 2). To gain information about this point, a computational analysis based on the three crystal structures presented in this paper was performed to explain this particular behavior of CX-5011. In particular, a double-mutant (V66I174AA) model and the two single-mutant (V66A and I174A) models were built in silico and used to perform a set of docking experiments with compounds CX-4945, CX-5011, and CX-5279. The docking experiments (results summarized in Table 5) show that the incidence of the superimposable poses

Table 5. Incidence of Superimposable Poses from Different Docking Experiments[a]

compd	CK2αWT	CK2α (V66I174AA)	CK2αWT (V66A)	CK2αWT (I174A)
CX-4945	67%	42%	44%	65%
CX-5011	75%	72%	71%	72%
CX-5279	72%	36%	32%	47%

[a]The reported values represent the means obtained from five independent experiments with the standard deviation never exceeding 2%.

for compound CX-5011 is absolutely constant both in wild-type CK2α and in the case of single and double mutants. CX-4945, instead, seems to be sensitive to the double mutant (42%) and mutant V66A (44%), but not to mutant I174A (65%). Finally, CX-5279 is shown to be quite sensitive to double and single mutants. CX-5011 (but not CX-4945) can take advantage of the interaction between water molecule W3 and the nitrogen atom (A1) of its pyrimidine ring in a zone hydrophobically controlled by V66. Therefore, in the case of CX-5011, the V66A mutation is compensated by this unique interaction with W3. This water molecule, present in both CX-4945 and CX-5011 crystal structures but not in that of CX-5279, is hydrogen bonded to Asn118 and to the phenylamino NH group of both CX-4945 and CX-5011. Moreover, in the case of CX-5011, W3 is responsible for a third interaction with the nitrogen atom (A1) of the pyrimidine ring. This latter contact seems to play a key role in maintaining the IC_{50} of CX-5011 at low levels even in the presence of single and double mutants. As shown in Table 2, while both CX-4945 and CX-5011 are almost insensitive to I174A mutations (IC_{50} = 3.51 and 2.50 nM, respectively), CX-4945 is shown to be quite sensitive to the V66 to Ala mutation (IC_{50} = 13.5 nM). On the other hand, the unique interaction of W3 with nitrogen A1 of CX-5011 seems to ensure a tight binding of the compounds also in the absence of Val66 [IC_{50} = 2.32 nM (see Table 2)]. In the case of CX-5279, this unique water molecule cannot be accommodated in the crystal structure, because of the bulky presence of the cyclopropane ring. This probably explains why CX-5279 is the most sensitive to both single and double mutations with respect to CX-4945 and CX-5011 (see Table 2). In conclusion, the computational analysis supported by biochemical data allows us to explain the different behaviors of compounds whose structures are superimposable in their complexes with CK2.

CONCLUSION

We have experimentally determined the features underlying the interaction between CK2 and a novel class of highly potent and selective ATP-competitive inhibitors. Their particularly high potency results both from the hydrophobic effect due to the transfer of a highly apolar molecule in an essentially hydrophobic environment (the ATP-binding site) and from the optimal coupling of the ligand polar moieties (important for solubility) to protein counterparts, mainly the positive electrostatic area near the conserved water W1 and Lys68, and the backbone of the hinge region. This is one of the few cases in which CK2 inhibitors can simultaneously bind to the hinge region and to Lys68. Important for the binding is also the shape complementarity (van der Waals contribution) between the ligands and the active site of CK2, particularly small for the presence of bulky residues such as gatekeeper residue Phe113, and the unique Val66 and Ile174. Some polar interactions between inhibitors and CK2 are mediated by a network of water molecules clearly visible in the high-resolution crystal structures, in the solvent-exposed side of the ligands. In the case of CX-5011, which is insensitive to double mutations in the ATP-binding site, enhanced interaction with water molecules appears to compensate for mutations of key binding site amino acids such as Val66, an unexpected and unprecedented observation with known CK2 inhibitors. This work rationalizes the observed enzymological inhibition of CK2 and provides a firm experimental confirmation of previous SAR studies.

The kinase selectivity profile of CX-4945 and analogues CX-5011 and CX-5279 showed that they are more selective for CK2 than any previously described inhibitor, including quinalizarin and the most widely used pharmacological tools, TBB and DMAT. Of particular interest is the observation that modification of the scaffold ring directly interacting with the hinge region, through addition of nitrogen atoms in the heterocyclic framework or substitution with small alkyl amino moieties, resulted in a significant improvement in selectivity and higher Gini coefficients. This result provides important information about the optimization of future classes of inhibitors that would interact with the same region of the enzyme.

Evidence that the pharmacological inhibition of CK2 bears great promise for the treatment of various ailments is provided by the progression of CX-4945 through clinical trials for cancer.[27] This novel class of tricyclic inhibitors with high potency and the highest selectivity for CK2 ever reported offers

an unprecedented set of powerful tools to help unravel the cellular functions of the multifunctional protein kinase CK2.

■ ASSOCIATED CONTENT

Supporting Information

Selectivity profiles of CX-4945, CX-5011, and CX 5279 against panels of 102 and 235 protein kinases (Tables S1–S6), $2F_O$-F_C electron density map of inhibitor CX-4945 in complex with human CK2α contoured at 2σ level (Figure S1), ATP-dependent inhibition of CK2α by CX-5011 (Figure S2A), and the K_i values derived from the apparent K_i values generated using the Morrison equation replotted against ATP (Figure S2B). This material is available free of charge via the Internet at http://pubs.acs.org.

Accession Codes

Coordinates and structure factors have been deposited in the Protein Data Bank as entries 3PE1 (human CK2–CX-4945), 3PE2 (human CK2–CX-5011), and 3R0T (human CK2–CX-5279).

■ AUTHOR INFORMATION

Corresponding Author

*R.B.: Department of Chemical Sciences, University of Padova, Via Marzolo 1, 35131 Padova, Italy, and Venetian Institute of Molecular Medicine (VIMM), Via G. Orus 2, 35129 Padova, Italy; telephone, +39 049 8275265 and +39 049 8275239; fax, +39 049 8275829; e-mail, roberto.battistutta@unipd.it. F.P.: Cylene Pharmaceuticals, Inc., 5820 Nancy Ridge Dr., Suite 200, San Diego, CA 92121; telephone, (858) 875-5113; fax, (858) 875-5101; e-mail, fpierre@cylenepharma.com. L.A.P.: Department of Biological Chemistry, University of Padova, Viale G. Colombo 3, 35131 Padova, Italy; telephone, +39 049 8276108; fax, +39 049 8073310; e-mail, lorenzo.pinna@unipd.it.

Funding

This work was supported by grants from Associazione Italiana per la ricerca sul Cancro (AIRC) and Italian Ministry of University (PRIN 2008) to L.A.P. and R.B.

■ ACKNOWLEDGMENTS

We thank the staff at beamline XDR1 of the ELETTRA Synchrotron Light Source for on-site assistance in data collection. The Molecular Modelling Section (MMS) coordinated by Professor S. Moro (Padova, Italy) is gratefully acknowledged.

■ ABBREVIATIONS

CK2, casein kinase 2; PIM1, provirus integration site for Moloney murine leukemia virus.

■ REFERENCES

(1) Salvi, M., Cesaro, L., Tibaldi, E., and Pinna, L. A. (2010) Motif analysis of phosphosites discloses a potential prominent role of the Golgi casein kinase (GCK) in the generation of human plasma phospho-proteome. *J. Proteome Res. 9*, 3335–3338.

(2) Meggio, F., and Pinna, L. A. (2003) One-thousand-and-one substrates of protein kinase CK2? *FASEB J. 17*, 349–368.

(3) Pinna, L. A. (2003) The raison d'etre of constitutively active protein kinases: The lesson of CK2. *Acc. Chem. Res. 36*, 378–384.

(4) Pinna, L. A. (2002) Protein kinase CK2: A challenge to canons. *J. Cell Sci. 115*, 3873–3878.

(5) Pagano, M. A., Marin, O., Cozza, G., Sarno, S., Meggio, F., Treharne, K. J., Mehta, A., and Pinna, L. A. (2010) Cystic fibrosis transmembrane regulator fragments with the Phe508 deletion exert a dual allosteric control over the master kinase CK2. *Biochem. J. 426*, 19–29.

(6) Litchfield, D. W. (2003) Protein kinase CK2: Structure, regulation and role in cellular decisions of life and death. *Biochem. J. 369*, 1–15.

(7) Ruzzene, M., Di Maira, G., Tosoni, K., and Pinna, L. A. (2010) Assessment of CK2 constitutive activity in cancer cells. *Methods Enzymol. 484*, 495–514.

(8) Ahmad, K. A., Wang, G., Unger, G., Slaton, J., and Ahmed, K. (2008) Protein kinase CK2: A key suppressor of apoptosis. *Adv. Enzyme Regul. 48*, 179–187.

(9) Di Maira, G., Brustolon, F., Bertacchini, J., Tosoni, K., Marmiroli, S., Pinna, L. A., and Ruzzene, M. (2007) Pharmacological inhibition of protein kinase CK2 reverts the multidrug resistance phenotype of a CEM cell line characterized by high CK2 level. *Oncogene 26*, 6915–6926.

(10) Kramerov, A. A., Saghizadeh, M., Caballero, S., Shaw, L. C., Li Calzi, S., Bretner, M., Montenarh, M., Pinna, L. A., Grant, M. B., and Ljubimov, A. V. (2008) Inhibition of protein kinase CK2 suppresses angiogenesis and hematopoietic stem cell recruitment to retinal neovascularization sites. *Mol. Cell. Biochem. 316*, 177–186.

(11) Ruzzene, M., and Pinna, L. A. (2010) Addiction to protein kinase CK2: A common denominator of diverse cancer cells? *Biochim. Biophys. Acta 1804*, 499–504.

(12) Solimini, N.L., Luo, J., and Elledge, S. J. (2007) Non-oncogene addiction and the stress phenotype of cancer cells. *Cell 130*, 986–988.

(13) Tawfic, S., Yu, S., Wang, H., Faust, R., Davis, A., and Ahmed, K. (2001) Protein kinase CK2 signal in neoplasia. *Histol. Histopathol. 16*, 573–582.

(14) Wang, G., Unger, G., Ahmad, K. A., Slaton, J. W., and Ahmed, K. (2005) Downregulation of CK2 induces apoptosis in cancer cells: A potential approach to cancer therapy. *Mol. Cell. Biochem. 274*, 77–84.

(15) Piazza, F. A., Gurrieri, C., Trentin, L., and Semenzato, G. (2007) Towards a new age in the treatment of multiple myeloma. *Ann. Hematol. 86*, 159–172.

(16) Silva, A., Yunes, J. A., Cardoso, B. A., Martins, L. R., Jotta, P. Y., Abecasis, M., Nowill, A. E., Leslie, N. R., Cardoso, A. A., and Barata, J. T. (2008) PTEN posttranslational inactivation and hyperactivation of the PI3K/Akt pathway sustain primary T cell leukemia viability. *J. Clin. Invest. 118*, 3762–3774.

(17) Kim, J. S., Eom, J. I., Cheong, J. W., Choi, A. J., Lee, J. K., Yang, W. I., and Min, Y. H. (2007) Protein kinase CK2α as an unfavorable prognostic marker and novel therapeutic target in acute myeloid leukemia. *Clin. Cancer Res. 13*, 1019–1028.

(18) Wang, G., Ahmad, K. A., and Ahmed, K. (2005) Modulation of death receptor-mediated apoptosis by CK2. *Mol. Cell. Biochem. 274*, 201–205.

(19) Sarno, S., and Pinna, L. A. (2008) Protein kinase CK2 as a druggable target. *Mol. BioSyst. 4*, 889–894.

(20) Battistutta, R. (2009) Protein kinase CK2 in health and disease: Structural bases of protein kinase CK2 inhibition. *Cell. Mol. Life Sci. 66*, 1868–1889.

(21) Battistutta, R., Sarno, S., De Moliner, E., Papinutto, E., Zanotti, G., and Pinna, L. A. (2000) The replacement of ATP by the competitive inhibitor emodin induces conformational modifications in the catalytic site of protein kinase CK2. *J. Biol. Chem. 275*, 29618–29622.

(22) Battistutta, R., De Moliner, E., Sarno, S., Zanotti, G., and Pinna, L. A. (2001) Structural features underlying selective inhibition of protein kinase CK2 by ATP site-directed tetrabromo-2-benzotriazole. *Protein Sci. 10*, 2200–2206.

(23) Prudent, R., and Cochet, C. (2009) New protein kinase CK2 inhibitors: Jumping out of the catalytic box. *Chem. Biol. 16*, 112–120.

(24) Pagano, M. A., Bain, J., Kazimierczuk, Z., Sarno, S., Ruzzene, M., Di Maira, G., Elliott, M., Orzeszko, A., Cozza, G., Meggio, F., and Pinna, L. A. (2008) The selectivity of inhibitors of protein kinase CK2: An update. *Biochem. J. 415*, 353–365.

(25) Duncan, J. S., Gyenis, L., Lenehan, J., Bretner, M., Graves, L. M., Haystead, T. A., and Litchfield, D. W. (2008) An unbiased evaluation

of CK2 inhibitors by chemoproteomics: Characterization of inhibitor effects on CK2 and identification of novel inhibitor targets. *Mol. Cell. Proteomics 7*, 1077−1088.

(26) Pierre, F., Chua, P. C., O'Brien, S. E., Siddiqui-Jain, A., Bourbon, P., Haddach, M., Michaux, J., Nagasawa, J., Schwaebe, M. K., Stefan, E., Vialettes, A., Whitten, J. P., Chen, T. K., Darjania, L., Stansfield, R., Anderes, K., Bliesath, J., Drygin, D., Ho, C., Omori, M., Proffitt, C., Streiner, N., Trent, K., Rice, W. G., and Ryckman, D. M. (2011) Discovery and SAR of 5-(3-Chlorophenylamino)benzo[c][2,6]-naphthyridine-8-carboxylic Acid (CX-4945), the First Clinical Stage Inhibitor of Protein Kinase CK2 for the Treatment of Cancer. *J. Med. Chem. 54*, 635−654.

(27) Siddiqui-Jain, A., Drygin, D., Streiner, N., Chua, P., Pierre, F., O'Brien, S. E., Bliesath, J., Omori, M., Huser, N., Ho, C., Proffitt, C., Schwaebe, M. K., Ryckman, D. M., Rice, W. G., and Anderes, K. (2010) CX-4945, an orally bioavailable selective inhibitor of protein kinase CK2, inhibits prosurvival and angiogenic signaling and exhibits antitumor efficacy. *Cancer Res. 70*, 10288−10298.

(28) Padgett, C. S., Lim, J. K. C., Marschke, R. F., Northfelt, D. W., Andreopoulou, E., Von Hoff, D. D., Anderes, K., Ryckman, D. M., Kung Chen, T., and O'Brien, S. E. (2010) Clinical Pharmacokinetics and Pharmacodynamics of CX-4945, a Novel Inhibitor of Protein Kinase CK2: Interim Report from the Phase 1 Clinical Trial. 22nd EORT-NCI-AACR Symposium, Berlin, Poster 414.

(29) Pierre, F., O'Brien, S. E., Haddach, M., Bourbon, P., Schwaebe, M. K., Stefan, E., Darjania, L., Stansfield, R., Ho, C., Siddiqui-Jain, A., Streiner, N., Rice, W. G., Anderes, K., and Ryckman, D. M. (2011) Novel potent pyrimido[4,5-c]quinoline inhibitors of protein kinase CK2: SAR and preliminary assessment of their analgesic and anti-viral properties. *Bioorg. Med. Chem. Lett. 21*, 1687−1691.

(30) Ferguson, A. D., Sheth, P. R., Basso, A. D., Paliwal, S., Gray, K., Fischmann, T. O., and Le, H. V. (2011) Structural basis of CX-4945 binding to human protein kinase CK2. *FEBS Lett. 585*, 104−110.

(31) Copeland, R. A. (2000) *Enzymes, a Practical Introduction to Structure, Mechanism, and Data Analysis*, 2nd ed., pp 310−315, Wiley-VCH, New York.

(32) Graczyk, P. P. (2007) Gini coefficient: A new way to express selectivity of kinase inhibitors against a family of kinases. *J. Med. Chem. 50*, 5773−5779.

(33) Kabsch, W. (2010) Xds. *Acta Crystallogr. D66*, 125−132.

(34) Collaborative Computational Project, Number 4 (1994) 1994The CCP4 suite: Programs for protein crystallographyActa Crystallogr.

(35) McCoy, A. J., Grosse-Kunstleve, R. W., Adams, P. D., Winn, M. D., Storoni, L. C., and Read, R. J. (2007) Phaser crystallographic software. *J. Appl. Crystallogr. 40*, 658−674.

(36) Emsley, P., Lohkamp, B., Scott, W. G., and Cowtan, K. (2010) Features and development of Coot. *Acta Crystallogr. D66*, 486−501.

(37) Adams, P. D., Afonine, P. V., Bunkoczi, G., Chen, V. B., Davis, I. W., Echols, N., Headd, J. J., Hung, L. W., Kapral, G. J., Grosse-Kunstleve, R. W., McCoy, A. J., Moriarty, N. W., Oeffner, R., Read, R. J., Richardson, D. C., Richardson, J. S., Terwilliger, T. C., and Zwart, P. H. (2010) PHENIX: A comprehensive Python-based system for macromolecular structure solution. *Acta Crystallogr. D66*, 213−221.

(38) Cozza, G., Mazzorana, M., Papinutto, E., Bain, J., Elliott, M., di Maira, G., Gianoncelli, A., Pagano, M. A., Sarno, S., Ruzzene, M., Battistutta, R., Meggio, F., Moro, S., Zagotto, G., and Pinna, L. A. (2009) Quinalizarin as a potent, selective and cell-permeable inhibitor of protein kinase CK2. *Biochem. J. 421*, 387−395.

(39) Sarno, S., de Moliner, E., Ruzzene, M., Pagano, M. A., Battistutta, R., Bain, J., Fabbro, D., Schoepfer, J., Elliott, M., Furet, P., Meggio, F., Zanotti, G., and Pinna, L. A. (2003) Biochemical and three-dimensional-structural study of the specific inhibition of protein kinase CK2 by [5-oxo-5,6-dihydroindolo-(1,2-a)quinazolin-7-yl]acetic acid (IQA). *Biochem. J. 374*, 639−646.

(40) Niefind, K., Raaf, J., and Issinger, O. G. (2009) Protein kinase CK2 in health and disease: Protein kinase CK2: From structures to insights. *Cell. Mol. Life Sci. 66*, 1800−1816.

(41) Traxler, P., and Furet, P. (1999) Strategies toward the design of novel and selective protein tyrosine kinase inhibitors. *Pharmacol. Ther. 82*, 195−206.

(42) Ladbury, J. E., and Doyle, M. L., Eds. (2004) *Biocalorimetry 2: Applications of calorimetry in the biological sciences*, John Wiley & Sons, New York.

(43) Meggio, F., Deana, A. D., and Pinna, L. A. (1981) Endogenous phosphate acceptor proteins for rat liver cytosolic casein kinases. *J. Biol. Chem. 256*, 11958−11961.

(44) Pagano, M.A., Andrzejewska, M., Ruzzene, M., Sarno, S., Cesaro, L., Bain, J., Elliott, M., Meggio, F., Kazimierczuk, Z., and Pinna, L. A. (2004) Optimization of protein kinase CK2 inhibitors derived from 4,5,6,7-tetrabromobenzimidazole. *J. Med. Chem. 47*, 6239−6247.